CRYO / 02 / 030
December, 13, 2002

Flower, a Model for the Analysis of Hydraulic Networks and Processes

L. Bottura, C. Rosso

Distribution: Internal

Presented: Workshop on Computation of Thermo-Hydraulic Transients in Superconductors, Karlsruhe, 15-18 September, 2002

Published: to appear in Cryogenics, 2003

Summary

We have developed in the past years a model that describes hydraulic networks that are typical of the cryogenic interconnection of superconducting magnets. The original model, called Flower, was used mostly to provide consistent boundary conditions for the operation of a magnet. The main limitations were associated with the number and nature of modelling elements available, and to the maximum size of the model that could be solved. Here we present an improvement of the model largely relaxing the above limitations by the addition of new modelling elements, such as parallel flow heat exchangers, and by a significant improvement in the numerics of the solver, using sparse matrix storage and solution techniques. We finally show a typical application to the case of a magnet quench in the LHC string.

Introduction

Cryogenic systems used for cooling superconducting magnets are complex assemblies of passive and active hydraulic components, including mainly piping, manifolds, valves, pumps and turbines. In most conditions the time scale of the typical response of a cryogenic system is longer than the time scale characterising transients in magnetic systems. Still in many practical situations the steady state and transient response of the proximity cryogenics strongly affects the behaviour of the magnet, e.g. during cool-down or a during a quench. In turn the whole cryogenic system responds to transient conditions in the magnet through regulating or safety actions. The interplay among systems is difficult to predict and a common, conservative approach is to assume that the magnetic systems and the cryogenic systems operate independently. This is realised setting ideal boundary conditions for the magnet (e.g.

constant pressure and temperature helium inlet during normal operation) as well as for the cryogenic system (e.g. the massflows and temperature of coolant from a quenching coil necessary to size the quench relief lines).

When optimized operation is important, or when the conservative approach described above results in excessive safety or engineering margins, it is however interesting to proceed one step further in the representation of the whole system, integrating the cryogenic and magnetic system in a whole and studying the combined transient and steady state response for the *load cases* of interest. Of course in an undertaking of this type it is mandatory to introduce simplifications in the representation of the systems, dropping the details in the corresponding models.

We have started an approach of this type in our early development of a tool, Flower [1-3], coupled to a thermo-hydraulic simulation model for a superconducting cable in a coil, Gandalf [4]. The original model [1] was based on a simplified technique for the assembly of manifolds, pipes, valves and pumps, the *hydraulic network*, and provided pressure, temperature and massflow conditions to the coil inlet and outlet. In its original version, the main limitations were associated to the number and nature of modelling elements available, and to the maximum size of the model that could be solved. We have improved on these drawbacks, largely relaxing the above limitations by the addition of new modelling elements, such as heat exchangers, and by a significant improvement in the numerics of the solver, using sparse matrix storage and solution techniques.

In the form described here the hydraulic network can be extended to model the proximity cryogenic *as well as* the cooling circuits of the coil. The rationale behind this approach is to provide a single integrated tool for the design and analysis of cooling systems with complex topology, focussing on the thermo-hydraulics of the system. Issues such as temperature margin, current sharing, or quench propagation are regarded as secondary and can be taken into account by suitable approximations during the simulation of the overall thermo-hydraulic response of a system.

In this paper we present the details of the model presently implemented in Flower, we discuss the solution technique selected and we present some examples of application.

Model

A typical cryogenic system can be regarded in first approximation as an assembly of active and passive components forming an *hydraulic network.* We consider the network as composed of:

- interconnected junctions where the flow can be steady state or transient. Junctions can be of different type, passive (e.g. a pipe or a valve) or active (e.g. a pump or a turbine);
- volume nodes with perfect mixing of helium and zero flow, representing buffers and manifolds.

In the model definition we assume further that junctions always interconnect volume nodes. Volumes, however, can have negligible size so that the result is a direct interconnection of two (or more) juntions in the same point. The junction definitions are based on the following types included in the model:

- 1-D flow pipes, including full compressible flow and propagation delay and waves,
- valves, with concentrated head loss and isenthalpic flow,
- pumps (volumetric or centrifugal), with isentropic flow,
- turbines, also with isentropic flow.

In addition the model considers thermal links among 1-D flow pipes, as e.g. in the case of heat exchange between parallel flows, among 1-D pipes and volumes, as would be the case for heat exchange between a pipe submerged in a bath, and among volumes.

Figure 1 shows a schematic representation of a possible hydraulic network. In the next sections we write the equations that form the basis of the model. Throughout this paper we will consider only single phase helium flow. We are aware that this poses strong limitations in the analysis of a complete cryogenic system, where phase separation processes are commonly taking place. We have considered however that treating two phase flow from the start would lead to a model very hard to manage and use. Nonetheless, should the need arise, we believe that the method for the solution of the equations discussed here could be extended to deal with two-phase flow.

Volume

A volume represents either a physical buffer, a manifold or a point where two or more junctions are interconnected. In this point the flow velocity is not defined, and is assumed to be zero. The equations to be solved for a volume are the balances of mass and energy conservation. For the *k*-th volume V_k the two equations in integral form are:

$$V_k \frac{\partial \rho_k}{\partial t} + \sum \dot{m}_i = 0 \tag{1}$$

$$V_k \frac{\partial \rho_k i_k}{\partial t} + \sum \dot{m}_i \left(h_i + \frac{v_i^2}{2} \right) = \dot{q}_k \tag{2}$$

where ρ_k is the density and i_k is the specific internal energy of the fluid. The internal specific energy instead of the total energy has been used in the balance Eq. (2) because we have assumed zero velocity. The sum of the massflows $\dot{m}_i$ and of the stagnation enthalpy flux $\dot{m}_i \left(h_i + \frac{v_i^2}{2} \right)$ is intended over all the in- and outflow surfaces of the

volume, and thus spans the set of junctions connected to the volume. Finally, $\dot{q}_k$ is the heating power in the volume from external sources and from thermal links (see later).

The form for the mass and energy balances given above was used in [1]. The major drawback of this form is that mass and energy fluxes in the junctions connecting volumes are driven by pressure gradients. Pressure, however, does not appear explicitly in the equations. Therefore the evaluation of the fluxes and their influence on the pressure in the volume nodes required an iterative procedure that in several cases could fail to converge. For this reason, we follow here a different approach. We use the following relations among thermodynamic variables involving the Gruneisen parameter f, the isentropic sound speed c and the specific heat at constant volume C_v:

$$dr = \frac{1+f}{c^2}dp - \frac{fr}{c^2}dh \tag{3}$$

$$di = \frac{1}{r}\left(\frac{p}{r} - fC_vT\right)dr - C_v dT \tag{4}$$

to transform by simple algebra Eqs. (1) and (2) into the following equations for the volume node pressure and temperature (see [5] and [4] for details):

$$V_k \frac{\P p_k}{\P t} + \sum_i r_i A_i v_i \left[c_k^2 + f_k\left(h_i + \frac{v_i^2}{2} - h_k\right)\right] = f_k \dot{q}_k \tag{5}$$

$$V_k r_k C_k \frac{\P T_k}{\P t} + \sum_i r_i A_i v_i \left(f_k C_k T_k + h_i + \frac{v_i^2}{2} - h_k\right) = \dot{q}_k \tag{6}.$$

Compressible flow pipe

Pipings in the proximity cryogenics, the cooling circuit of a magnet, or a force-flow cooled superconducting cable can be regarded as compressible flow pipes. For this reason we consider in the model the general case of a compressible flow pipe with flow cross section A_i, hydraulic diameter D_i, wetted perimeter w_i, friction factor f_i, heat transfer coefficient h_i and heating power density $\dot{q}_i'$ deposited either from the external or through thermal links. For this junction we write the descriptive equations using the velocity, pressure and temperature (v_i,p_i,T_i) as state variables:

$$\frac{\partial v_i}{\partial t} + v_i \frac{\partial v_i}{\partial x} + \frac{1}{r_i}\frac{\partial p_i}{\partial x} + 2\frac{f_i}{D_i} v_i |v_i| = 0 \tag{7}$$

$$A_i \frac{\partial p_i}{\partial t} + A_i r_i c_i^2 \frac{\partial v_i}{\partial x} + A_i v_i \frac{\partial p_i}{\partial x} - 2A_i f_i \frac{f_i}{D_i} r_i v_i^2 |v_i| = f_i \dot{q}_i' + f_i \dot{q}_{cf,i}' \tag{8}$$

$$r_i C_i A_i \frac{\partial T_i}{\partial t} + r_i C_i A_i f T_i \frac{\partial v}{\partial x} + r_i C_i A_i v \frac{\partial T_i}{\partial x} - 2A_i \frac{f_i}{D_h} r_i v_i^2 |v_i|_i = \dot{q}_i' + \dot{q}_{cf,i}' \tag{9}.$$

The equations above provide a complete and exact description of compressible flow in the pipe for any coolant. See Ref. [4] for more details on the derivation. The term $\dot{q}'_{cf,i}$ models the counterflow heat exchange in Helium II [6] and appears as a diffusion-like contribution for operation in helium below the lambda temperature T_λ given by:

$$\dot{q}'_{cf,i} \approx A_i \frac{\partial}{\partial x}\left(\frac{F(T_i, p_i)^{1/3}}{\left(\frac{\partial T_i}{\partial x}\right)^{2/3}} \frac{\partial T_i}{\partial x} \right) \tag{10}$$

where the effective conductivity function $F(T,p)$ is a property tabulated from experimental data. The details on how to deal with this term can be found in [7, 8].

The system of Eqs. (7)-(10) is discretized in space using a first-order accurate finite element method, giving rise to a system of ordinary differential equations in time. The procedure used for the discretization has been extensively discussed in [4]. Boundary conditions are needed at the two ends of the pipe. For subsonic flow the boundary conditions depend on the direction of the flow and on the fluid state. For the case of inflow the boundary pressure and temperature are imposed at the end of the pipe. For the case of outflow in normal fluid conditions only pressure is prescribed at the pipe end, while in superfluid conditions also the temperature is imposed. The boundary values of temperature and pressure correspond to those of the volumes connected to the inlet and outlet of the pipe. The case of supersonic flow is not relevant for the analysis of cryogenic systems in normal operation and is therefore not addressed here.

For the solution of the balances in the volumes connected at the pipe inlet and outlet it is necessary to evaluate the massflow and enthalpy at the corresponding location in the pipe. The calculation of the massflow at the boundary of the pipe is straightforward:

$$\dot{m}_i = A_i \rho_i v_i \tag{11}$$

and the enthalpy can be computed using tabulated properties for the fluid:

$$h_i = h(T_i, p_i) \tag{12}$$

where the quantities v_i, T_i and p_i are obtained from the solution of the pipe equations at the appropriate location (inlet or outlet).

Steady state flow valve

A valve acts on the flow causing a pressure drop that can be approximated in the incompressible case as:

$$\Delta p \approx -2\chi\rho v|v| \tag{13}$$

where we call x the *head loss factor* which can be computed from the known valve characteristic K_v and valve cross section A using the following approximation [9]:

$$x \approx 6.5\times10^{8}\left(\frac{A}{K_v}\right)^2 \tag{14}.$$

The valve characteristic can be, in general, a function of the flow and fluid state in the valve. Although in reality the flow in a valve can be extremely complex, especially in transient conditions, we make here the assumption that the valve reaches steady state conditions much faster than the time scales of interest for the system. In this case the massflow is constant at any section in the valve (although it can still be time dependent), and is given by:

$$\dot{m}_i = a\left(p_k - p_h\right) \tag{15}$$

where the valve connects volumes h and k and positive flow is conventionally taken from inlet to outlet. The *flow coefficient* a appearing above is given by:

$$a = A\sqrt{\frac{1}{2x}\frac{\overline{r}}{\left|p_h - p_k\right|}} \tag{16}.$$

Here and in the following the overbar quantities are intended as *upwinded* (i.e. computed from the values upstream). For any quantity y this means that:

$$\overline{y} = \begin{cases} y_h & for\ \dot{m} \geq 0 \\ y_k & for\ \dot{m} < 0 \end{cases} \tag{17}.$$

Finally, the flow through the valve is assumed to take place without energy input, is therefore at constant enthalpy and we can write:

$$h_i = \overline{h} \tag{18}.$$

Equations (15) and (18) provide the description of the flow in the valve needed for the network analysis. Various situations can be considered depending on the flow and pressure drop dependence of the head loss factor $x = x\left(\dot{m}, p_h, p_k, T_h, T_k\right)$. Control valves can have a continuous dependence, while check valves or burst disks can be strongly non-linear, with the limit case that $x \to \infty$ and a=0 in the case of a closed valve. A sample of possible cases are given in Fig. 2. As exemplified there, the valve characteristics can depend on the flow as well as on the flow direction, and can exhibit hysteretic behaviour, as, e.g., a burst disk after rupture. We have checked that all the non-linear cases reported in Fig. 2 can be dealt with by the solver described later.

Volumetric pump

A volumetric pump is modelled as a component that provides a given massflow under any possible operating conditions, i.e. with a horizontal characteristic in the pressure head-massflow operating plane as shown in Fig. 3:

$$\dot{m}_i = \dot{m}_0 \tag{19}$$

where $\dot{m}_0$ is the prescribed massflow. To evaluate the change in the fluid state from inlet to outlet we take the flow in the volumetric pump as isentropic. We use the thermodynamic relation:

$$dh = TdS + \frac{1}{r}dp \tag{20}$$

where S is the entropy and in our case dS=0. The enthalpy change across the pump is then given by the following approximation:

$$\Delta h_i = \int_{p_h}^{p_k} \frac{1}{r}dp \approx \frac{1}{2}\left(\frac{1}{r_h} + \frac{1}{r_k}\right)\left(p_k - p_h\right) \tag{21}$$

that corresponds to an increase in enthalpy for the normal situation when the pump compresses and increases the fluid pressure (i.e. $p_k > p_h$). Equations (19) and (21) provide the necessary description of the flow.

Compressor

For a compressor we choose the following approximation of the massflow characteristic:

$$\dot{m}_i = \begin{cases} \dot{m}_0\left(1 - \left(\dfrac{p_k - p_h}{\Delta p_0}\right)^2\right) & for\ p_k \geq p_h \\ \dot{m}_0 & for\ p_k < p_h \end{cases} \tag{22}$$

where the pump is oriented from volume h to volume k so that p_k - p_h is the pressure difference between outlet and inlet of the pump, the massflow $\dot{m}_0$ is delivered when there is no pressure difference at the extreme of the pumps, and Dp_0 is the maximum pressure head that can be sustained with zero mass flow. The characteristic above is plotted in Fig. 3. Note that the pump allows backflow in the case that the pressure difference from inlet to outlet is higher than the one sustained by the compressor.

As for the volumetric pump, we assume that the flow through the compressor is isentropic and we evaluate the enthalpy change from inlet to outlet using Eq. (21). Equations (22) and (21) provide the description of the flow as required by the model.

Turbine

The flow through a turbine can be taken in first approximation as limited by the hydraulic impedance of the succession of impellers and blades. We therefore take Eq. (14) for expressing the relation between pressure drop across the turbine and the turbine flow:

$$\Delta p \approx -2x_T\, r v|v| \tag{23}$$

where the head loss factor x_T is characteristic of the turbine. The peculiarity of the flow in the turbine is however that a large part of the thermal energy (and to a lesser extent kinetic energy) is transformed in work. The amount of work performed depends on the thermodynamic transformation of the fluid through the turbine. As for pump and compressor, we make the assumption of ideal, isentropic flow through the turbine. Similarly to above, Eq. (21) provides the change in fluid enthalpy across the turbine. In this case, as opposed to the pump, the pressure decreases from inlet to outlet and the corresponding enthalpy change is negative.

Thermal links

We consider three possible cases for thermal links among components: between two volumes filled with stagnant fluid, between two pipes in co-current or counter-current flow and between a volume with stagnant fluid and a pipe with flowing fluid.

Thermal link between two volumes

The power exchanged between two volumes h and k linked thermally through a thermal resistance R_{hk} depends only on the temperature difference between volumes, and can be writen as follows:

$$\dot{q}_{hk} = \frac{1}{R_{hk}}\left(T_h - T_k\right) \tag{24}$$

where the thermal resistance R_{hk} has units of [K/W]. In Eq. (24) we have neglected for simplicity the heat transfer coefficient at the wall of the volume containment structure, that is considered already taken into account in the definition of R_{hk}. The power given by Eq. (24) is added during the network assembly process to the external power in the volume k, in Eqs. (5) and (6). The power $\dot{q}_{kh}$ from volume k to volume h is identical in module to Eq. (23), but opposite in sign, and must be added to the equations for volume h.

Thermal link between two pipes

Two pipes j and i, thermally linked, exchange power depending on the local value of the temperature gradient between the two pipes, on the heat transfer coefficient

between fluid flow and pipe wall, and on the thermal resistivity per unit length r_{ji} between the pipe walls, in units of [K/Wm]. We can express the local power per unit length as:

$$\dot{q}'_{ji} = \frac{1}{\frac{1}{w_j h_j} + r_{ji} + \frac{1}{w_i h_i}} \left(T_j - T_i\right) \tag{25}.$$

The power given by Eq. (25) is added to the external power in Eqs. (8) and (9) for the pipe *i*, as well as in the equations for pipe *j* (with opposite sign).

Thermal link between a pipe and a volume

The power exchanged between a pipe *i* and a volume *k* is using Eq. (25) and integrating over the length of the pipe. As in the case of two volumes we neglect heat transfer in the volume itself, so that the power per unit length of the pipe is given by:

$$\dot{q}'_{ki} = \frac{1}{r_{ji} + \frac{1}{w_i h_i}} \left(T_k - T_i\right) \tag{26}$$

and is added to the external power in Eqs. (8) and (9) for the pipe *i*. The power in the volume is obtained from:

$$\dot{q}_{ik} = \int_L \frac{1}{r_{ji} + \frac{1}{w_i h_i}} \left(T_k - T_i\right) dx \tag{27}$$

which is added to the external power in the volume *k*, in Eqs. (5) and (6).

Network assembly and solution

To solve an arbitrary assembly of hydraulic components as described in the previous sections it is necessary to proceed to a *network assembly*, producing matrix equations to be solved in time to advance the system state from a known initial condition. The matrix equations are obtained:

- assigning the same degree-of-freedom to the pressure and temperature of inlet and outlet of steady state junctions (valves, pumps, compressors, turbines) and the volumes respectively connected;

- imposing boundary conditions on pressure and inlet temperature of the compressible flow pipes, taking as boundary values those from the connected volumes;

- coupling the in- and outflows of all junction types (including compressible flow pipes) to the mass and energy fluxes in the connected volume nodes;

- coupling the temperature and pressure degrees-of-freedom in correspondance to thermal links across the network.

The system to be solved has the form:

$$\mathbf{M}(\mathbf{U})\frac{\partial \mathbf{U}}{\partial t} + \mathbf{A}(\mathbf{U})\mathbf{U} = \mathbf{Q}(\mathbf{U}) \tag{28}$$

and it consists of a set of ordinary differential equations in time for the unknown **U**, including pressure and temperature of the volumes of the network and for the velocity of the nodes of the compressible flow pipes. All other variables are eliminated during the network assembly process, thus reducing the number of unknowns to the minimum possible. The integration of Eq. (27) in time from time t^n to time t^{n+1} is performed using a first order, finite difference method:

$$\mathbf{M}\left(\mathbf{U}^{n+1}\right)\frac{\mathbf{U}^{n+1} - \mathbf{U}^{n}}{\Delta t} + \mathbf{A}\left(\mathbf{U}^{n+1}\right)\mathbf{U}^{n+1} = \mathbf{Q}\left(\mathbf{U}^{n+1}\right) \tag{29}.$$

where the implicit dependencies of the matrices **M**, **A** and the source vector **Q** are solved by fixed point iteration, with starting value given by the known solution at time t^n. The algorithm chosen has the desired numerical stability and robustness against the non-linear terms in **M**, **A** and **Q**. Note that given the large spectrum of time scales potentially present in the solution we have preferred a stable, low order numerical solution to high order algorithms with better error characteristics but much more prone to instabilities. The resulting algebraic system is solved implicitly, by matrix inversion at each time step.

In the case of practical network analysis the components used can be many and, as is the case of compressible flow pipes, can require several hundreds of nodes to model waves properly. As a consequence the system matrices can grow to a very large dimension, requiring large memory for storage an long execution times for inversion at each time step. To deal with this problem we have minimised the memory requirements by storing the system matrices in indexed, sparse format. In addition we use a generalised minimum residual (GMRES) method for the iterative solution of system Eq. (29) at each step. The GMRES is adapted to non-symmetric matrices and uses an incomplete LU factorization as pre-conditioner [10]. Generally few iterations are sufficient to achieve the matrix inversion to the machine precision, thus also increasing considerably the computational efficiency as compared to direct matrix inversion.

Example of application

As a typical example of application we have chosen to show how to simulate the thermohydraulics of an isolated magnet quench in the string model for the Large

Hadron Collider (LHC) that is presently under test at CERN [11]. The LHC String 2 consists presently of six dipole magnets (MB1 to MB6) and two short-straight sections containing each a defocussing and a focussing quadrupole (MQ1 and MQ2 respectively). The magnets are assembled in the sequence shown schematically in Fig. 4. Two relief valves at the two ends of the magnet string provide the safety discharge in case that the pressure increases above a preset value (usually set in the range of 17 to 18 bar). The string magnets have been quenched in a sequence of experiments devoted at verifying the response of the LHC local as well as distributed transitions to normal state. We have selected a particular run in which all dipoles were powered at nominal current, and the dipole MB3 was intentionally quenched.

To identify the modelling elements for the simulation of the LHC String 2 we have followed the approach described in [12] and [13]. Each magnet has been modelled as two volumes, of which the first represents the helium in intimate contact with the superconducting coil, heated during a quench, while the second volume represents the rest of the helium contained in the cold mass, between the iron laminations, in the end-caps and in the internal pipings. This is a much simplified version of the model described in [13], where in addition the presence and size of helium buffer volumes at the magnet endcaps as well as the time dependent temperature margin of the superconducting coil were modelled in a much greater detail.

The total helium inventory in a cold mass is approximately 20 l/m [12]. We have taken for the 15-m long dipoles a total volume of 315 l, and for the short-straight sections 186 l. Of this volume, 3 % was assigned to the helium in proximity of the coil and 97 % to the rest of the cold mass. The mass and energy exchange between the two volumes has been modelled interconnecting them with a pipe of large cross section, 0.18 m^2 for the dipoles and 0.06 m^2 for the short-straight sections, (corresponding to the gaps of the iron laminations with a filling factor of 98 % for the iron yoke) and linking them thermally through a constant heat transfer resistance, corresponding to a linear heat transfer coefficient of approximately 200 W/m K.

The magnets in the string are in communication through the piping at the interconnects. This has been modelled linking the cold mass helium volumes with short pipes (1 m length), with 50 cm^2 cross section, and adding a thermal resistance that simulates the heat flux transmitted by counter-flow mechanism in superfluid helium (i.e. at most 20 kW/m^2). Finally, the two relief valves were added to the network model, connected to the two volumes simulating the MQ1 and MB6 cold masses, at the extremities of the String 2. A schematic view of the model is shown in Fig. 5

The effect of a dipole quench was simulated by an external heating deposition in the volumes in proximity to the coil of a magnet. The heating waveform for the volume *k* associated with a quenching magnet was taken as:

$$\dot{q}_k = \dot{q}_{TR} e^{-\left(\frac{t-t_Q}{t}\right)} + \dot{q}_{SS} \qquad (30)$$

where $\dot{q}_{TR}$ (60 kW) is the power deposited during the transient, with a time constant t (30 s), while $\dot{q}_{SS}$ (6.5 kW) is the heating power in the subsequent, slow phase of heat transfer. The time t_Q corresponds to the beginning of the quench (see below). Equation (30) has resemblance to the measured power deposition profiles reported in [12] and [13] and the coefficients have been obtained fitting the curves reported there. Note that during a quench only a small part of the magnetic energy is deposited in the helium, while a large portion is stored in the thermal capacity of the cold mass. With the values taken above about 1/4 of the magnet energy is transferred to the helium during the first 2 minutes of the evolution.

The initial situation taken for the simulation was of superfluid operation at 1.9 K and 1 bar. Quench propagation from a magnet to the neighbouring one was triggered as soon as the helium temperature in the volume in proximity to the coil of a magnet increased above the lambda point. The rationale behind this assumption is that each magnet is described by a single helium mass and has therefore no detail on the distribution of temperature along the magnet length. The transition of the whole cold mass from superfluid to normal helium has been taken to indicate the arrival of the normal fluid front from the neighbouring, quenching magnet. This is associated in reality with a sharp temperature increase that was properly considered in [13], but is not modelled accurately by the simple model used for the demonstration calculation discussed here.

The results of the simulation performed are summarised in Figs. 6 and 7. With the choice of parameters and assumptions described above the model predicts well, within 5 seconds, the quench propagation from dipole MB3 to the dipoles MB2 and MB1 (see Fig. 6). The quench propagation time from dipole MB3 to the dipole MB4, taking place across the short straight section MQ2 (not powered during this experiment), is underestimated by about 15 s in the simulation. This is most probably due to the simplifications introduced in the model as compared to the inherent complexity of the hydraulic connections among magnets of different type as well as the neglect of the temperature distribution inside a magnet. The pressure evolution, in Fig. 7, follows the measured values, albeit with a 15 s delay in the time of the opening of the relief valves. The most probable explanation for this delay is the uncertainty in the exact amount of Joule heat deposited from the coil into the helium volumes. In summary, the results achieved with this simple model, aimed mainly at demonstrating the features of the network solver, appear as satisfactory for scoping studies and analyses of first order effects.

Conclusions

We have presented in this paper the details of a model suitable for the analysis of complex hydraulic networks. The main evolution of the model with respect to the situation described previously [1-3] is the definition of two new components, heat exchangers and turbines. In addition we have significantly improved the numerics of the solution algorithm using standard sparse matrix storage and system solution techniques. The example of application to the quench propagation in the LHC String 2 shows that a complex situation can be modelled to a satisfactory degree already with a

relatively simple assembly of hydraulic elements. Thus, in perspective, the model described in this paper aims mainly at the analysis of complete systems, allowing the study of the coupling of proximity cryogenics to the end user. Further extensions, e.g. cryoplant models, may require however significant improvement of the models of single components (e.g. pumps and turbines) and the proper description of two-phase thermo-hydraulics.

Acknowledgements

The data on the quench propagation in the LHC String II at CERN was kindly provided by L. Serio and C. Calzas Rodriguez (CERN). We gratefully acknowledge the contribution of the CERN LHC String Experimental Team in performing the tests, analysing the data and providing critical expertise on their evaluation.

References

[1] L. Bottura, *Quench Propagation through Manifolds in Forced Flow Cooled Coils*, IEEE Trans. Appl. Sup., **3**, 1, 606-609, 1993.

[2] L. Bottura, C. Rosso, *Hydraulic Network Simulator Model*, CryoSoft Internal Note, CRYO/97/004, 1997.

[3] C. Marinucci, L. Bottura, *The Hydraulic Solver Flower and its Validation Against the QUELL Experiment in SULTAN*, IEEE Trans. Appl. Sup., **9**(2), 616-619, 1999.

[4] L. Bottura, *A Numerical Model for the Simulation of Quench in the ITER Magnets*, Jour. Comp. Phys., **125**, 26-41, 1996.

[5] V. Arp, *Computer Analysis of Qench Transients in Force-Flow Cooled Superconductors for Large MHD Magnets*, Proc. of Superconducting MHD Magnet Design Conf., MIT, Cambridge, 1978.

[6] S.W. Van Sciver, *Helium Cryogenics*, Clarendon Press, 1986.

[7] A. Kashani, S.W. Van Sciver, J.C. Strikwerda, *Numerical Solution of Forced Convection Heat Transfer in He II*, Numerical Heat Transfer, **16**, Part A, 213-228, 1989.

[8] L. Bottura, C. Rosso, *Finite Element Simulation of Steady-State and Transient Forced Convection in Superfluid Helium*, Int. J. Num. Meth. Fluids, **30**, 1091-1108, 1999.

[9] L. Bottura, *K_v-value and Head Loss Factor in Control Valves*, CryoSoft Internal Note, CRYO/98/011, 1999.

[10] P.N. Brown, A.C. Hindmarsh, *Reduced Storage Matrix Methods in Stiff ODE Systems*, Lawrence Livermore National Laboratory Report, UCRL-95088, Rev. 1, 1987.

[11] F. Bordry, et al., *First Powering of the LHC Test String 2*, IEEE Trans. Appl. Sup., **12**(1), 232-235, 2002.

[12] M. Chorowski, P. Lebrun, L. Serio, R. van Weelderen, *Thermohydraulics of Quencehs and Helium Recovery in the LHC Prototype Magnet Strings*, Cryogenics, **38**, 533-543, 1998.

[13] M. Chorowski, P. Grzegory, L. Serio, R. van Weelderen, *Modelling of Helium-Mediated Quench Propagation in the LHC Prototype Test String-1*, Cryogenics, **40**, 585-591, 2000.

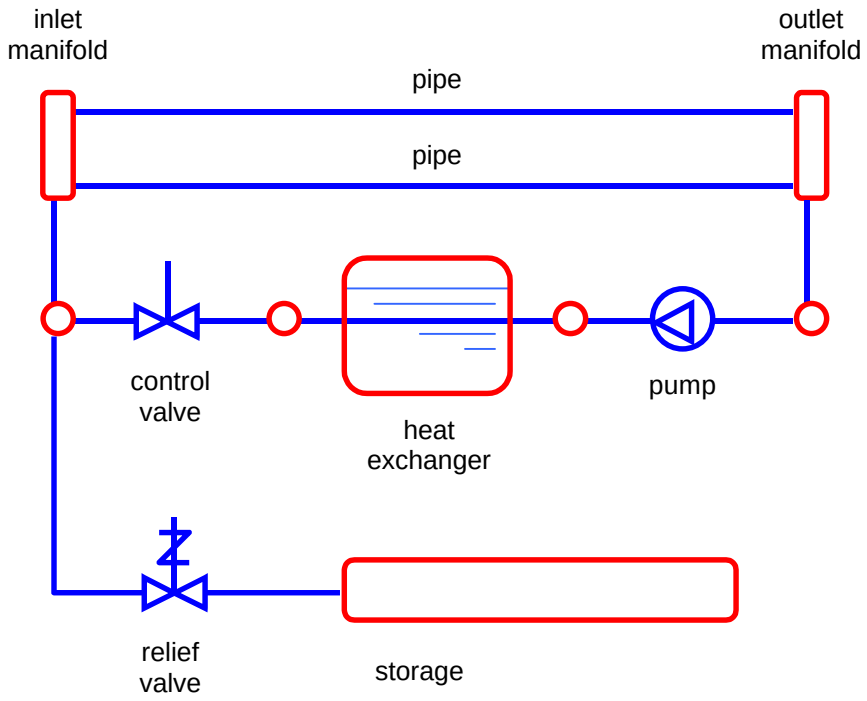

Figure 1. Schematic of an arbitrary network of passive and active hydraulic components. The system sketched is a simplified representation of a closed loop cooling system fed by a coolant flow generated by a pump and controlled in temperature by a heat exchanger. The relief valves open under a specified pressure and provide security against pressure increase.

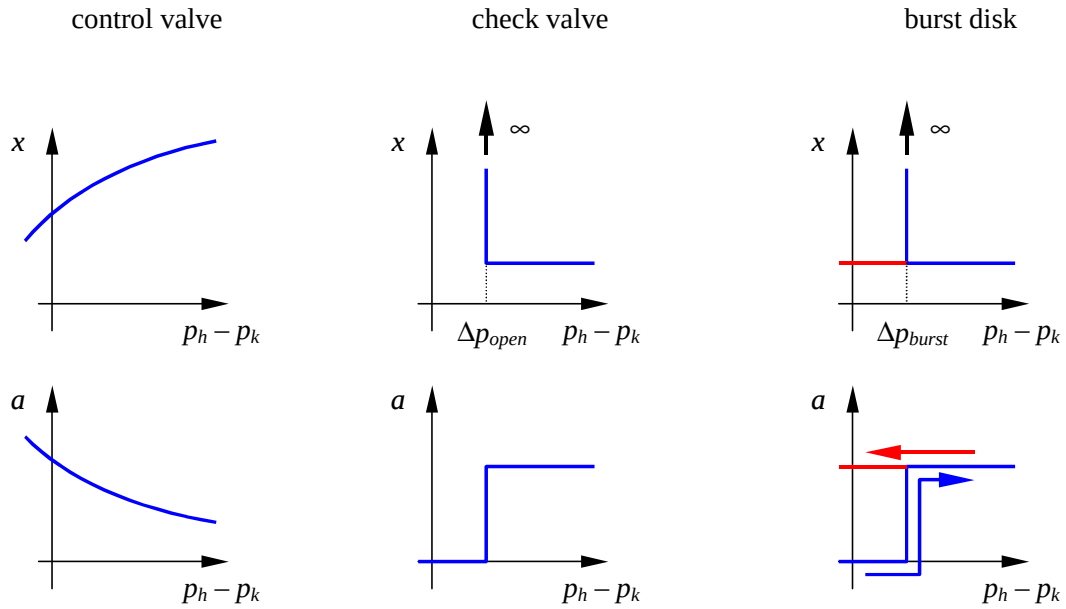

Figure 2. Head loss factor and flow coefficient for several possible cases corresponding to a control valve, a check valve and a burst disk. Note the hysteresis in the characteristic of the burst disk.

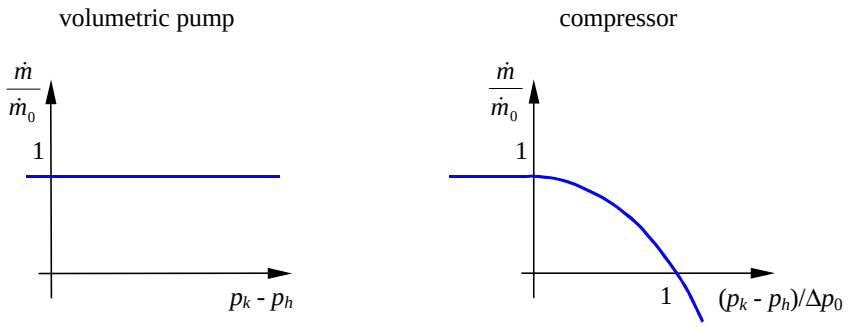

Figure 3. Pressure-head massflow characteristics of a volumetric pump and a compressor.

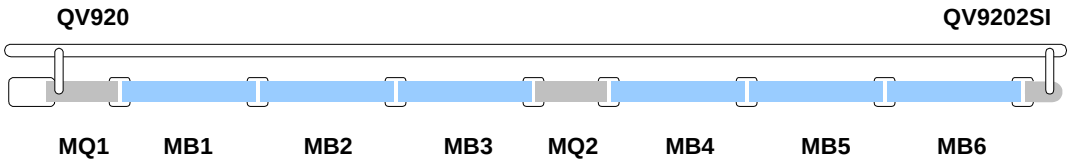

Figure 4. Schematic representation of the assembly of magnets forming String 2. The magnets are arc dipoles (MB1 through MB6) and Short Straight Sections containing the defocussing and focussing quadrupoles (MQ1 and MQ2 respectively). Also shown is the location of the two quench relief valves (QV920 and QV9202SI) and the helium line parallel to the string.

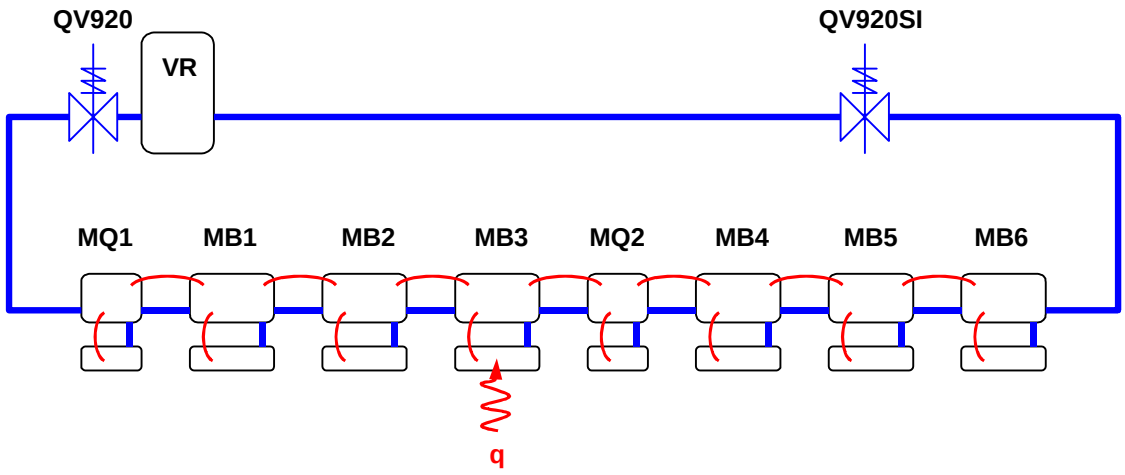

Figure 5. Model used for the simulation of quench thermo-hydraulics in String 2. The helium inventory in the single magnets is modelled using volumes interconnected hydraulically by pipes (straight connections) and thermally linked (arcs). The heating term in MB3 models the Joule heating during the magnet quench. Heating in the other magnets, function of temperature and time, is started as discussed in the text. The relief valves open at 17 bar in a large volume VR assumed to be at 6 bar.

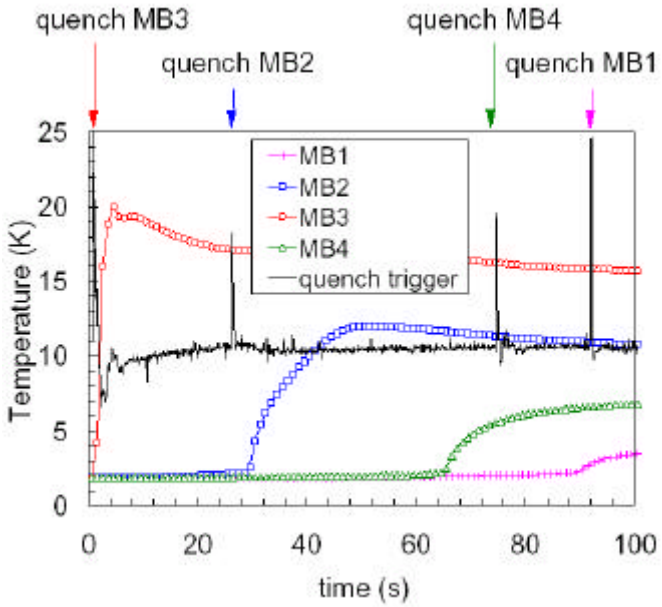

Figure 6. Evolution of the simulated helium temperature in the cold mass of selected magnets as compared to the quench trigger signal. The quench is assumed to happen in the simulation as soon as the average cold mass temperature is above the lambda-transition. The quench is initiated in dipole MB3. The time to quench the dipoles MB2 and MB1 is well matched by the simulation, while the time needed to quench the dipole MB4 is underestimated.

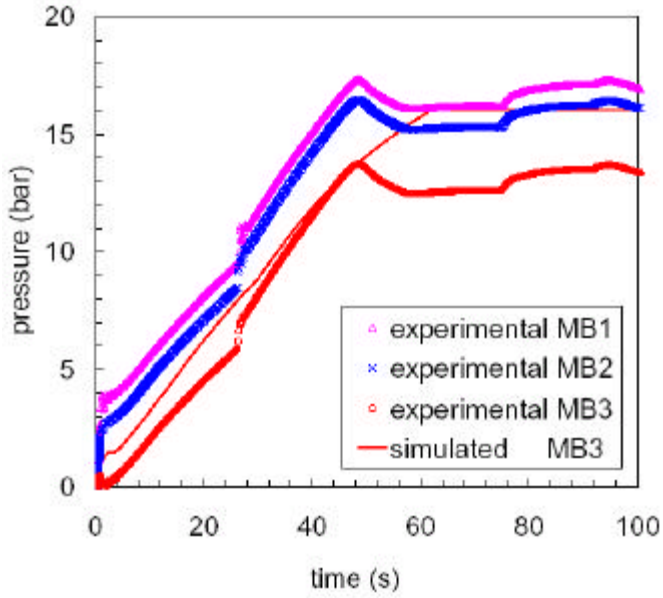

Figure 7. Evolution of the measured and simulated pressure in the LHC String-II during the quench of dipole MB3. The relief valve opens before 50 s in the experiment, and at about 65 s in the simulation.